The Journal of Immunology

Osteopontin Induces Ubiquitin-Dependent Degradation of STAT1 in RAW264.7 Murine Macrophages

Chengjiang Gao, Hongtao Guo, Zhiyong Mi, Michael J. Grusby and Paul C. Kuo

J Immunol 2007; 178:1870-1881; ;
doi: 10.4049/jimmunol.178.3.1870
http://www.jimmunol.org/content/178/3/1870

The Journal of Immunology is published twice each month by
The American Association of Immunologists, Inc.,
1451 Rockville Pike, Suite 650, Rockville, MD 20852

Print ISSN: 0022-1767 Online ISSN: 1550-6606.

Osteopontin Induces Ubiquitin-Dependent Degradation of STAT1 in RAW264.7 Murine Macrophages[1]

Chengjiang Gao,* Hongtao Guo,* Zhiyong Mi,* Michael J. Grusby,† and Paul C. Kuo[2]*

In systemic inflammation induced by endotoxin (LPS), the macrophage produces the majority of the circulating NO metabolites. However, while the molecular pathways which up-regulate iNOS expression have been extensively studied in the macrophage, little is known of the parallel counterregulatory pathways which repress or inhibit macrophage iNOS expression. Using both in vivo and in vitro murine models of endotoxin (LPS) stimulation, we have previously demonstrated that NO feedback inhibits its own synthesis by increasing transcription of osteopontin (OPN), a potent transrepressor of inducible NO synthase expression. In this current study, using a system of LPS-treated RAW264.7 macrophages, we go on to demonstrate that OPN increases STAT1 ubiquitination and subsequent 26s proteasome-mediated degradation to inhibit STAT1 dependent iNOS promoter activity, transcription, and protein expression. In addition, we identify STAT-interacting LIM protein as the critical STAT ubiquitin E3 ligase critical for STAT1 degradation in this setting. OPN has not been linked previously to STAT1 degradation. This regulation of STAT1 degradation underlies OPN′s effect as an inhibitor of iNOS gene transcription. These are novel findings and define OPN as a unique and as yet, poorly characterized, transactivator of STAT1 degradation by the ubiquitin-proteasome system. ***The Journal of Immunology,*** **2007, 178: 1870–1881.**

Macrophage-inducible NO synthase (iNOS)[3] expression is central to many of the systemic effects associated with endotoxin (LPS) stimulation (1). Using both in vivo and in vitro murine models of endotoxin (LPS) stimulation, we have previously demonstrated that NO feedback inhibits its own synthesis by increasing transcription of osteopontin (OPN), a potent transrepressor of iNOS expression (2–4). OPN transcription and promoter activity are significantly up-regulated in response to NO in LPS-stimulated ANA-1 and RAW264.7 murine macrophages (5). OPN gene transcription is regulated by a constitutive repressor protein, heterogeneous nuclear ribonucleoprotein (hnRNP)-A/B. Our findings suggest that LPS induced *S*-nitrosylation of hnRNP-A/B inhibits its activity as a constitutive repressor of the OPN promoter and results in enhanced OPN expression (3). In a subsequent study, we found that hnRNP-A/B and hnRNP-U proteins serve antagonistic transcriptional regulatory functions for OPN expression in the setting of LPS-stimulated NO synthesis (4). In this regard, STAT1 is an essential activator of LPS and/or proinflammatory cytokine-mediated iNOS transcription in murine, rat, and human cells (6, 7). All mammalian iNOS promoters contain several homologies with the IFN-γ-regulated STAT1α binding sites (GAS). Posttranslational modifications of STAT proteins, such as arginine methylation, acetylation, and ubiquitination, have also been suggested as important means to regulate STAT signaling. However, these mechanisms have been poorly defined to date (8, 9).

In the current study, we examine the OPN-dependent effector arm of this NO-regulated negative feedback loop. In murine macrophage models of LPS stimulation, OPN increases STAT1 ubiquitination and subsequent 26s proteasome-mediated degradation to inhibit STAT1-dependent iNOS promoter activity, transcription, and protein expression. In addition, we identify STAT-interacting LIM (SLIM) protein as the critical STAT ubiquitin (Ub) ligase (E3) critical for STAT1 degradation in this setting.

Materials and Methods

Materials

N-carbobenzoxyl-L-leucinyl-L-norleucinal (MG-132), cycloheximide, and M2 anti-FLAG agarose were purchased from Sigma-Aldrich. Recombinant mouse IFN-γ, OPN, and anti-mouse OPN Ab were purchased from R&D Systems. Abs directed against STAT1 p84/p91, β-actin, and Ub were obtained from Santa Cruz Biotechnology. Anti-STAT1 phosphotyrosine-701 was purchased from Cell Signaling Technology. Hemagglutinin (HA) mAb (3F10) was obtained from Roche Applied Science. Goat β-actin polyclonal Ab was obtained from Santa Cruz Biotechnology. Rabbit anti-mouse SLIM serum was described previously (10).

Plasmid constructs

Full-length STAT1 cDNA (U06924) was obtained by RT-PCR with the following primers: STAT1-F, 5′-ACGAAGCTTATGTCACAGTGGTTC GAGCTTCAG-3′, and STAT1-R, 5′-ACGAAGCTTTTACACTTCAGAC ACAGAAATCAAC-3′; the 2250-bp fragment was inserted into the pCMV-FLAG2 vector (Sigma-Aldrich). OPN cDNA (J04806) was amplified by RT-PCR with primers: OPN-F, 5′-CGCGAATTCCATGAGATT GGCAGTGATTTG-3′, and OPN-R, 5′-CGCGGATCCTTAGTTGACCT CAGAAGATG-3′; the 885-bp fragment was inserted into the mammalian

*Department of Surgery, Duke University Medical Center, Durham, NC 27710; and †Department of Immunology and Infectious Diseases, Harvard School of Public Health, Boston, MA 02115

Received for publication September 13, 2006. Accepted for publication November 14, 2006.

The costs of publication of this article were defrayed in part by the payment of page charges. This article must therefore be hereby marked *advertisement* in accordance with 18 U.S.C. Section 1734 solely to indicate this fact.

[1] This work was supported by National Institutes of Health Grants R01-GM65113 and R01-AI44629 (to P.C.K.) and R01-AI506296 (to M.J.G.).

[2] Address correspondence and reprint requests to Dr. Paul C. Kuo, 110 Bell Building, Duke University Medical Center, Box 3522, Durham, NC 27710. E-mail address: kuo00004@mc.duke.edu

[3] Abbreviations used in this paper: iNOS, inducible NO synthase; BMM, bone marrow macrophage; ChIP, chromatin immunoprecipitation; DN, dominant negative; E1, Ub-activating enzyme; E2, Ub-conjugating enzyme; E3, Ub ligase; GAS, IFN-γ-regulated STAT1α binding site; HA, hemagglutinin; hnRNP, heterogeneous nuclear ribonucleoprotein; MEF, murine embryonic fibroblast; OPN, osteopontin; P-STAT1, phosphorylated Tyr^{701} STAT1; PIAS, protein inhibitor of STAT; PVDF, polyvinylidene difluoride; Q-PCR, quantitative real-time PCR; siRNA, small interfering RNA; siRNA MM, mismatch hairpin siRNA; SLIM, STAT-interacting LIM; SOCS, suppressor of cytokine signaling; Tap1, transporter associated with Ag processing 1; Ub, ubiquitin.

expression vector pcDNA3.1/HisB (Invitrogen Life Technologies). HA-Ub plasmid was provided by Dr. D. Bohmann (University of Rochester, Rochester, NY). The PathDetect GAS *cis*-reporting vector was purchased from Stratagene. Ub and SLIM mutants were generated by using the QuikChange II Site-Directed Mutagenesis kit (Stratagene) and inserted into a pCMV expression vector. Luciferase reporter constructs bearing the mouse iNOS promoter (GenBank accession no. L09126) and the mouse transporter associated with Ag processing 1 (Tap1) promoter (GenBank accession no. AF027865) were constructed in the pGL3 vector (Promega).

Cell lines

RAW264.7 murine macrophages, COS-1 monkey kidney cells, wild-type, and $SLIM^{-/-}$ murine embryonic fibroblasts (MEF) and primary murine bone marrow macrophages (BMM) (gift from Dr. Y. He, Duke University, Durham, NC) were maintained at 37°C under 5% CO_2 in DMEM supplemented with 10% heat-inactivated FCS, 100 U/ml penicillin, and 100 μg/ml streptomycin. LPS (100 ng/ml) was added in the absence of FCS to induce NO synthesis. After incubation for the designated time period at 37°C in 5% CO_2, the cells or media were harvested for assays. All cell types produce iNOS and OPN in the setting of LPS stimulation. Bone marrow cells were isolated by lavage of excised femurs, washed in PBS, plated in DMEM with 0.2% BSA into two 100-mm tissue culture dishes, and allowed to adhere for 2 h at 37°C. After washing out nonadherent cells, cells are cultured in DMEM with 10% FBS and 20% L cell-conditioned medium (as a source of M-CSF) to generate confluent BMM.

RNA interference for OPN and SLIM

Using GenBank sequence NM_009263 for murine OPN cDNA and computer analysis software (Ambion), we selected a candidate sequence in the OPN cDNA sequence for RNA interference: 5′-AAGTCAGCTGGATG AACCAAG-3′. This 21-nt sequence exhibits no homology with other known mouse genes. Synthetic, annealed small interfering RNA (siRNA) oligonucleotides were synthesized chemically, and gel electrophoresis was purified and used during transient transfection experiments. In a similar fashion, a siRNA was selected for SLIM (GenBank accession no. NM_145978): 5′-AAGAUCCGACAGAGCGCCUCA-3′. A mismatch hairpin (siRNA MM) siRNA with limited homology to mouse genes served as the siRNA-negative control. We have successfully used this particular construct in previous OPN knockdown experiments (11).

Transient transfection analysis

DNA transfections were conducted in 12-well plates using LipofectAMINE. Briefly, 1×10^6 cells were plated on a 12-well plate and allowed to grow for 24 h before the transfection. Two micrograms of plasmid DNA and 2 μg of protamine sulfate diluted in OPTI-DMEM and 24 μg of LipofectAMINE diluted in OPTI-DMEM were combined and incubated at room temperature for 20 min. Cells with transfection reagents were incubated for 4 h at 37°C in a CO_2 incubator. Transfection medium was then replaced with DMEM containing 10% FBS. At least 24 h later, the medium was changed, and cells were treated, as described previously. To control transfection efficiency between groups, 0.1 μg of pRL-TK was added to each well. Cells were harvested in 0.4 ml of reporter lysis buffer (Promega), and dual luciferase reporter assays were performed by following the protocol provided by the manufacturer.

Immunoblot analysis

Cells were lysed in buffer (0.8% NaCl, 0.02 KCl, 1% SDS, 10% Triton X-100, 0.5% sodium deoxycholic acid, 0.144% Na_2HPO_4, and 0.024% KH_2PO_4 (pH 7.4)) and centrifuged at $12,000 \times g$ for 10 min at 4°C. Protein concentration was determined by absorbance at 650 nm using protein assay reagent. Cell lysate (50 μg/lane) were separated by SDS-12% PAGE, and the products were electrotransferred to polyvinylidene difluoride (PVDF) membrane (Amersham Biosciences). The membrane was blocked with 5% skim milk PBS-0.05% Tween 20 for 1 h at room temperature. After being washed three times, blocked membranes were incubated with primary Ab for 1 h at room temperature, washed three times in PBS-0.05% Tween 20, and incubated with HRP-conjugated secondary Ab for 1 h at room temperature. After an additional three times washing, bound peroxidase activity were detected by the ECL detection system (Amersham Biosciences). For secreted protein analysis, serum-free DMEM was collected after 24-h incubation and centrifuged at $600 \times g$ for 5 min to remove cellular material; the supernatant was then concentrated 100-fold through Ultrafree Centrifugal filters (Millipore).

Northern blot analysis

Total RNA was isolated using TRIzol reagent (Invitrogen Life Technologies). RNA samples (10 μg/lane) were fractionated by electrophoresis on a 1% agarose formaldehyde gel and transferred to Hybond-C nylon membrane (Amersham Biosciences). ^{32}P-labeled probes were based upon the murine cDNA sequences for iNOS (457 bp; GenBank accession no. XM147149) and Tap1 (600 bp; GenBank accession no. U60021). cDNA probes were constructed to bridge two contiguous exons and were prepared by random primer labeling, followed by purification using a Sephadex G-50 minicolumn (BioMax). Hybridization was performed at 42°C for 18 h in ULTRAhyb hybridization buffer (Ambion). Following hybridization, filters were washed twice and subjected to autoradiography using Fuji film for a period of 14 h. β-Actin was used as the housekeeping gene.

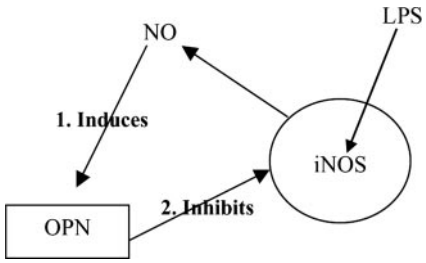

FIGURE 1. Relationships between OPN and iNOS in LPS-stimulated RAW264.7 murine macrophages.

Coimmunoprecipitation

Cells were washed with cold PBS and lysed for 15 min on ice in radioimmunoprecipitation assay lysis buffer (1× PBS, 1% Nonidet P-40, 0.5% sodium deoxycholate, and 0.1% SDS) containing protease inhibitors. Cell lysates were cleared by centrifugation (4°C, 20 min, 13,000 rpm). Aliquots (500 μg) were precleared by addition of 1.0 μg of normal IgG and 20 μl of appropriate agarose conjugate for 1 h. After centrifugation, the supernatant was collected and incubated with 2 μg of corresponding Ab for 1 h at 4°C with gentle rocking, then 20 μl of appropriate agarose conjugate was added and the mixture incubated overnight. After washing five times with lysis buffer, immunoblotting was performed as described previously.

Pulse and pulse-chase studies

Cells were incubated in medium without methionine and cysteine for 15 min. [^{35}S]Methionine/cysteine (100 μCi/ml) was added and incubated for the times indicated. The cells were lysed using Nonidet P-40 lysis buffer consisting of 150 mM NaCl, 50 mM Tris (pH 7.4), 40 mM NaF, 5% Nonidet P-40, and 10 mM Na_3VO_4. For pulse-chase analysis, the protocol was altered to re-expose cells to complete medium with excess methionine (10 mM) and cysteine (3 mM) and allowed to incubate. Equal amounts of total protein were immunoprecipitated with Ab, resolved by SDS-PAGE, transferred to PVDF, and exposed to x-ray film.

Quantitative real-time PCR (Q-PCR)

Total RNA was isolated by using the TRIzol reagent. First-strand complementary DNA was produced by reverse transcription of 1 μg total RNA using Superscript II (Invitrogen Life Technologies). Q-PCR was conducted using the iCycler thermocycler (Bio-Rad) in a final volume of 25 μl containing 1× QuantiTect SYBR buffer (Bio-Rad) and 0.4 μM primers. Amplification conditions were as follows: 95°C for 3 min, 40 cycles of 95°C for 30 s, 60°C for 30 s, and 72°C for 30 s. Actin was used to standardize the levels of cDNA. Serial dilutions (4-fold) of cDNAs were used to generate curves of log input amount vs threshold cycle and comparable slopes for a given primer set (signifying comparable efficiencies of amplification). The primer sequences used in Q-PCR assays are: iNOS, 5′-CAGATCC CGAAACGCTTCA, and iNOS, 3′-TGTTGAGGTCTAAAGGCTCCG; β-actin, 5′-AGGTGTGCACCTTTTATTGGTCTCAA, and β-actin, 3′-TG TATGAAGGTTTGGTCTCCCT; and Tap1, 5′-TTATCTTGGATGATGC CACCAG, and Tap1, 3′-AAGAAGAACCGTCCGAGAAGC.

To quantify each target transcript, a standard curve was constructed with serial dilutions of standard plasmid. After PCR, a melting curve analysis was performed to demonstrate the specificity of the PCR product as a single peak. A control, which contained all the reaction components (except for the template), was included in all experiments. The amount of each mRNA (iNOS and Tap1) was then normalized to a housekeeping gene, β-actin.

Chromatin immunoprecipitation (ChIP) assay

Chromatin from macrophages was fixed and immunoprecipitated using the ChIP assay kit (Upstate Biotechnology) as recommended by the manufacturer. Sequences were identified for the mouse iNOS promoter (GenBank

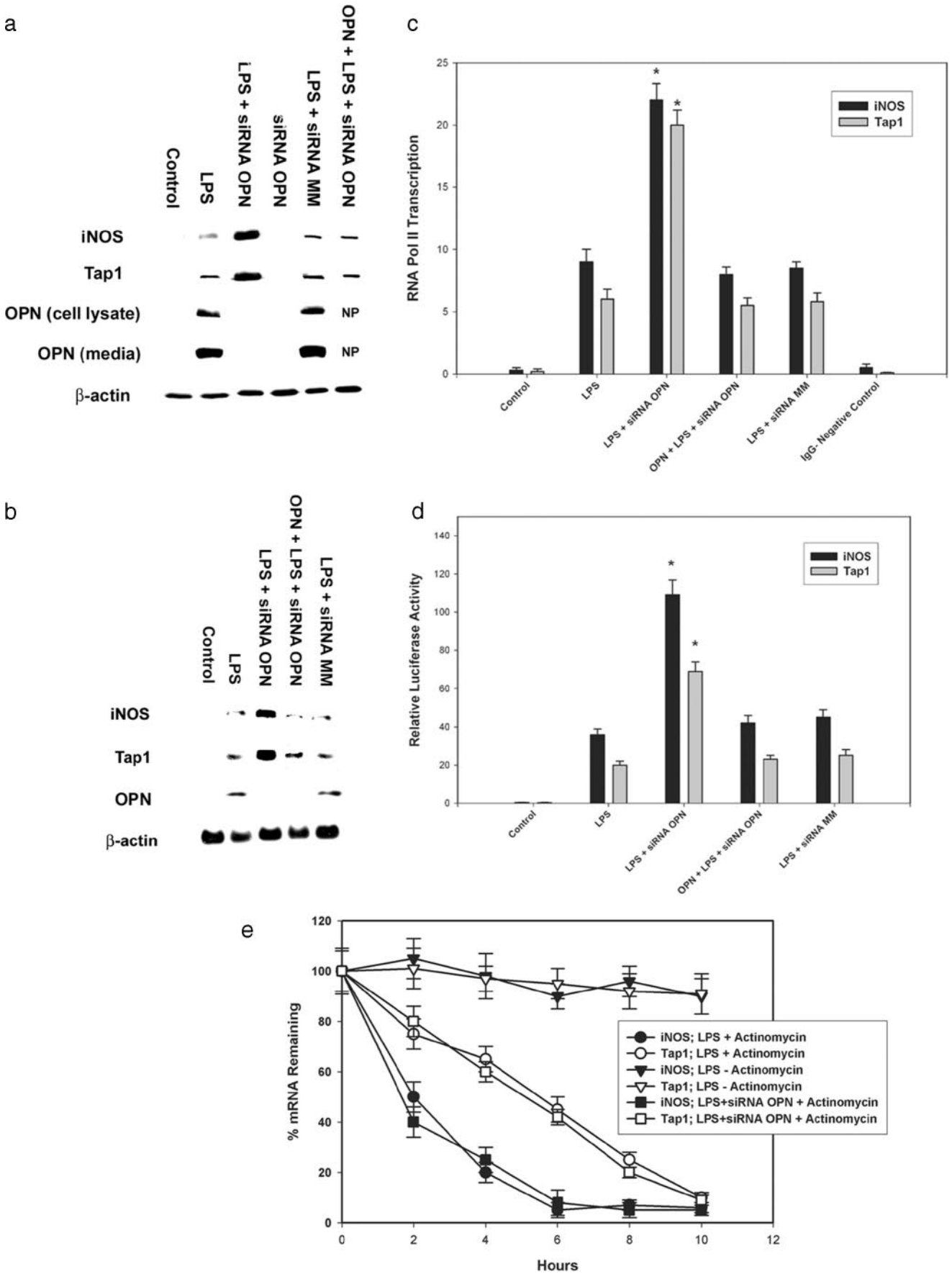

FIGURE 2. *a*, Immunoblot analysis of iNOS, Tap1, and OPN protein in RAW264.7 macrophages. Cells were transiently transfected with siRNA OPN or the mismatch control siRNA MM for 24 h. In selected instances, cells were then exposed to LPS (100 ng/ml) for 6 h in the presence of absence of OPN (50 μM). Unstimulated cells served as controls. Membranes were incubated with primary Ab to iNOS, Tap1, OPN, and β-actin followed by HRP-conjugated

accession no. L09126) and the mouse Tap1 promoter (GenBank accession no. AF027865). Purified chromatin was immunoprecipitated using 10 μg of anti-RNA Pol II (Abcam) or 5 μl of rabbit immune serum; eluted DNA fragments were purified to serve as templates. Murine iNOS or Tap1 promoter regions coimmunoprecipitating with RNA polymerase II were then quantified by real-time PCR using primers specific for each promoter region inclusive of the TATA start site (iNOS: forward, GTGTTGGAATAT TGGCACCA, and reverse, CGACGGTCCCAGTG, 390 bp; Tap1: forward, GGCTCGGCTTTCCAATCA, and reverse, GAGCGTGAGTGTCC AGAGTCT, 557 bp). Serial dilutions of genomic DNA were used to generate standard curves for real-time PCR using the corresponding primer sets. Copy numbers of the eluted promoter were normalized against the copy numbers in the corresponding inputs and expressed in arbitrary units. The input fraction corresponded to 0.1 and 0.05% of the chromatin solution before immunoprecipitation. After DNA purification, the presence of the selected DNA sequence was assessed by PCR. The PCR product was 338 bp in length. The PCR program was: 94°C × 4 min, followed by 94°C × 45 s, 55°C × 45 s, and 72°C × 45 s for a total of 28 cycles and then 72°C × 7 min. PCR products were resolved in 10% acrylamide gels.

ChIP-real-time PCR assay for NF-κB and STAT1 binding in iNOS and Tap1 promoters

Chromatin from macrophages was fixed and immunoprecipitated using the ChIP assay kit (Upstate Biotechnology) as recommended by the manufacturer. Sequences were identified for the mouse iNOS promoter (GenBank accession no. L09126) and the mouse Tap1 promoter (GenBank accession no. AF027865). Purified chromatin was immunoprecipitated using 10 μg of anti-NF-κB p65 (Santa Cruz Biotechnology), anti-STAT1 (Santa Cruz Biotechnology), or 5 μl of rabbit nonimmune serum; eluted DNA fragments were purified to serve as templates. The input fraction corresponded to 0.1 and 0.05% of the chromatin solution before immunoprecipitation. The average size of the sonicated DNA fragments subjected to immunoprecipitation was 500 bp as determined by ethidium bromide gel electrophoresis. After DNA purification, the presence of the selected DNA sequence was quantified by RT-PCR. ChIP assays addressing NF-κB-1 used the PCR primers TGTACCTTAGACAAGGCAAAACA and TGAGTTCT AGGACAAACTAGGGCT, resulting in a 260-bp fragment, whereas NF-κB-2 used AAACTGCAAATGAGAGAACAGACAG and TGTTTTGC ATAAAGTCACTGTTCC, resulting in a 312-bp fragment. ChIP assays for iNOS GAS used primers ACACGAGGCTGAGCTGACTT and CACACA TGGCATGGAATTTT, resulting in a 186-bp fragment. In Tap1, for GAS1 amplification, the primers GGAAGTAGGCGTTATCTAGTGAGC and GC CGAGTCCTCCCCTACT were used for a 210-bp fragment, while for GAS2, the primers AGATCTGCCCCGAGACAAGT and TAGCAAGC GTGGAAATCAGA resulted in a 210-bp fragment also.

Nuclear extract preparation

Monolayers of RAW264.7 cells were washed with PBS and harvested by scraping into cold PBS. The cell pellet obtained by centrifugation was resuspended in buffer containing 10 mM HEPES (pH 7.9), 10 mM KCl, 0.1 mM EDTA, 0.1 mM EGTA, 1.0 mM DTT, and 0.5 mM PMSF, then 10% Nonidet P-40 was added and vortexed briefly, and the nuclei were pelleted by centrifugation. Nuclear proteins were extracted with buffer containing 20 mM HEPES (pH 7.9), 0.4 mM NaCl, 1.0 mM EDTA, 1.0 mM EGTA, 1.0 mM DTT, and 1.0 mM PMSF. Insoluble material was removed by centrifugation at 14,000 rpm, and the supernatant containing the nuclear proteins was stored at 80°C until use.

Gel shift assays

Gel shift assays were performed using nuclear cell extract fraction, as described previously. In specific competitive binding assays, unlabeled oligonucleotides were added at 200 M excess. Probe was prepared by end-labeling double-stranded oligonucleotides with [^{32}-P]ATP (2500 Ci/mmol) using T4 polynucleotide kinase, followed by G-50 column purification. The reactions were resolved on a 6% nondenaturing acrylamide gel in 1× Tris-borate-EDTA buffer. All oligonucleotides used in the gel shift are HPLC grade.

In vitro ubiquitination assay

Recombinant His-tagged SLIM or empty His-vector was expressed in COS-1 cells and purified with MagneHis Protein Purification System (Promega) to use as the source of E3 ligase. Presence of SLIM was confirmed by rabbit anti-SLIM Ab. FLAG-tagged STAT1 was expressed in RAW264.7 cells, purified with M2 anti-FLAG agarose, and used as the source of substrate for in vitro ubiquitination. Briefly, anti-FLAG/STAT1 immunoprecipitates were washed five times with lysis buffer, once with ubiquitination buffer (50 mM Tris-Cl (pH 7.5), 2 mM $MgCl_2$, 2 mM ATP, and 1 mM DTT) and incubated in 40 μl of ubiquitination buffer with 5 μg of $(His)_6$-Ub, 100 ng of Ub-activating enzyme (E1), and 100 ng of GST-UbcH5a (Calbiochem) in the absence or presence of recombinant SLIM for 3 h at 30°C. After in vitro ubiquitination, all samples were washed three times with lysis buffer, eluted with SDS-sample buffer, resolved by SDS-PAGE, and transferred electrophoretically to PVDF membrane. STAT1 ubiquitination was detected by mouse anti-HisG Ab (Invitrogen Life Technologies).

Statistical analysis

Data are expressed as means ± SE. Analysis was performed using Student's t test. Values of $p < 0.05$ were considered significant.

Results

OPN inhibition of iNOS and Tap1 protein and mRNA expression

Our previous work has focused upon the NO regulated pathway by which OPN is up-regulated in the setting of LPS-mediated iNOS expression (step 1; Fig. 1). We have identified *S*-nitrosylation of hnRNP and the interchange between hnRNP-A/B and -U at the OPN promoter as primary regulators of NO-dependent OPN transcription (3, 4). In this current study, we will examine the OPN-dependent effector arm of this NO-regulated negative feedback loop (step 2; Fig. 1).

As an initial step, we examined the relationship between OPN expression and STAT1-dependent protein expression in LPS (100 ng/ml)-stimulated RAW264.7 murine macrophages. Immunoblot analysis (Fig. 2*a*) for OPN and the STAT1-dependent proteins,

secondary Ab. OPN content was measured in cell lysate and medium. The blot is representative of three experiments (NP, Not performed). *b*, Northern blot analysis of iNOS, Tap1, and OPN mRNA in RAW264.7 macrophages. Cells were transiently transfected with siRNA OPN or the mismatch control siRNA MM for 24 h. In selected instances, cells were then exposed to LPS (100 ng/ml) for 6 h in the presence of absence of OPN (50 μM). Unstimulated cells served as controls. The blot is representative of three experiments. *c*, Combined ChIP-real-time PCR assay for iNOS and Tap1 gene transcription. Cells were transiently transfected with siRNA OPN or the mismatch control siRNA-MM for 24 h. In selected instances, cells were then exposed to LPS (100 ng/ml) for 6 h in the presence of absence of OPN (50 μM). Unstimulated cells served as controls. Chromatin from macrophages was fixed and immunoprecipitated using anti-RNA Pol II or rabbit immune serum; eluted DNA fragments were purified to serve as templates. Murine iNOS or Tap1 promoter regions coimmunoprecipitating with RNA polymerase II were then quantified by real-time PCR using primers specific for each promoter region inclusive of the TATA start site. Serial dilutions of genomic DNA were used to generate standard curves for real-time PCR using the corresponding primer sets. Copy numbers of the eluted promoter were normalized against the copy numbers in the corresponding inputs and expressed in arbitrary units. Data are presented mean ± SEM of four experiments (*, $p < 0.01$ LPS+siRNA OPN vs LPS, LPS+siRNA MM, and OPN+LPS+siRNA OPN for iNOS and Tap1). *d*, Transient transfection analysis of iNOS and Tap1 promoter activation. Cells were transiently transfected with siRNA OPN or the mismatch control siRNA MM for 24 h. Then, cells underwent repeat transfection with iNOS or Tap1 promoter-luciferase plasmid constructs. At least 24 h later, the medium was changed. In selected instances, cells were then exposed to LPS (100 ng/ml) for 6 h in the presence of absence of OPN (50 μM). Unstimulated cells served as controls. Data are presented mean ± SEM of four experiments (*, $p < 0.01$ LPS+siRNA OPN vs LPS, LPS+siRNA MM, and OPN+LPS+siRNA OPN for iNOS and Tap1). *e*, Half-life of iNOS and Tap1 mRNA. RAW264.7 cells were transiently transfected with siRNA OPN for 24 h. The medium was changed, and cells were then exposed to LPS (100 ng/ml) for 6 h. Actinomycin D (50 μg/ml) was then added to inhibit global gene transcription. Northern blots were then performed at selected time intervals. Levels of mRNA were normalized to total cell protein and mRNA expression at time of actinomycin treatment (time 0). The graph is representative of three experiments.

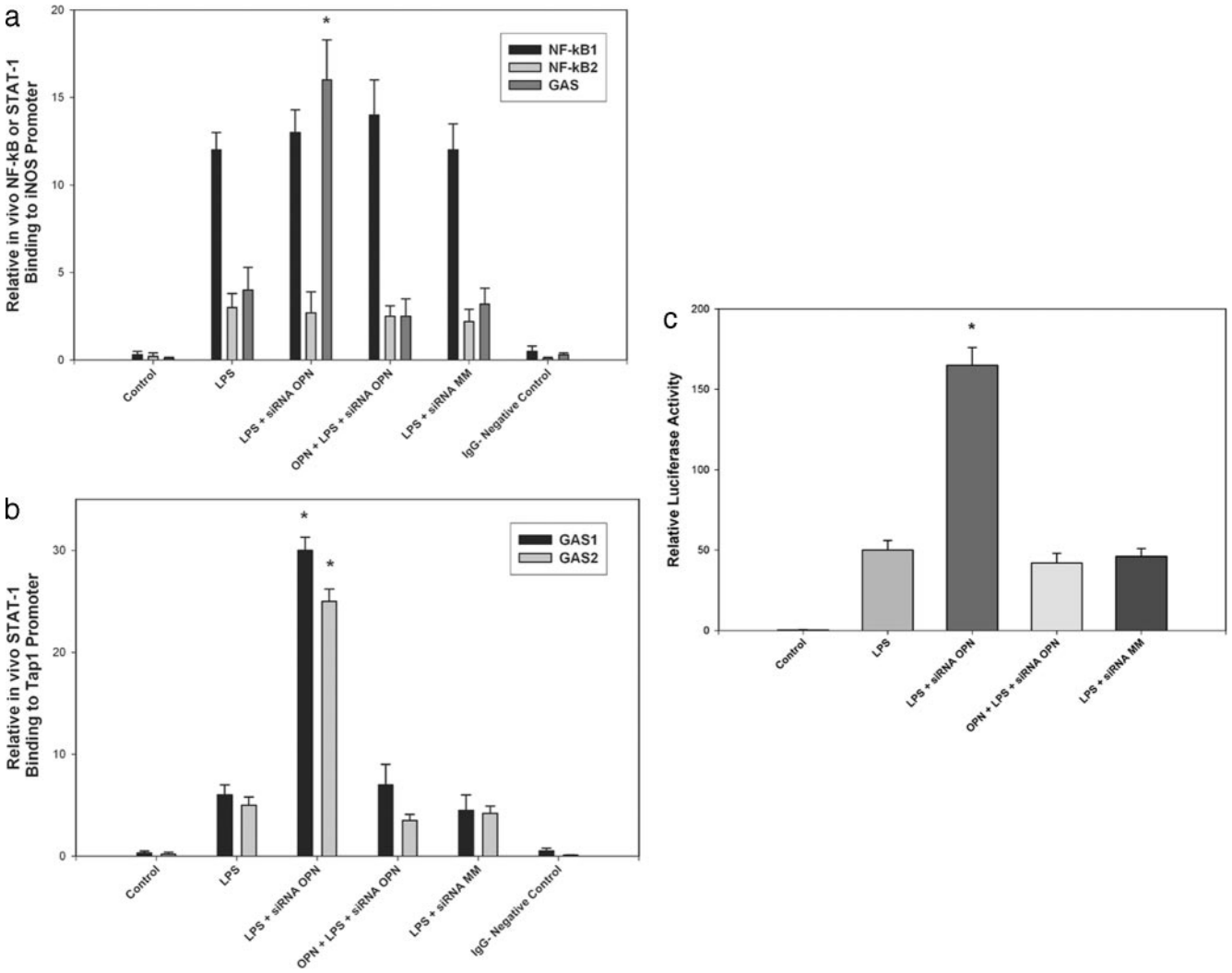

FIGURE 3. *a*, NF-κB and STAT1 in vivo binding to the iNOS promoter. Cells were transiently transfected with siRNA OPN or the mismatch control siRNA MM for 24 h. In selected instances, cells were then exposed to LPS (100 ng/ml) for 6 h in the presence of absence of OPN (50 μM). Unstimulated cells served as controls. Purified chromatin was immunoprecipitated using anti-NF-κB p65, anti-STAT1, or 5 μl of rabbit immune serum; eluted DNA fragments were purified to serve as templates. The presence of the selected DNA sequence was quantified by RT-PCR. Data are presented mean ± SEM of four experiments (*, $p < 0.01$ for STAT1 binding to GAS in LPS+siRNA OPN vs LPS, LPS+siRNA MM, and OPN+LPS+siRNA OPN for iNOS). *b*, STAT1 in vivo binding to the Tap1 promoter. Cells were transiently transfected with siRNA OPN or the mismatch control siRNA MM for 24 h. In selected instances, cells were then exposed to LPS (100 ng/ml) for 6 h in the presence or absence of OPN (50 μM). Unstimulated cells served as controls. Data are presented mean ± SEM of four experiments (*, $p < 0.01$ for STAT1 binding to GAS1 or GAS2 in LPS+siRNA OPN vs LPS, LPS+siRNA MM, and OPN+LPS+siRNA OPN for Tap1). *c*, Transient transfection analysis of consensus GAS promoter activity. Cells were transiently transfected with siRNA OPN or the mismatch control siRNA MM for 24 h. Then, cells underwent repeat transfection using a pGL3 luciferase reporter plasmid construct bearing a quadruple repeat of the GAS enhancer element. At least 24 h later, the medium was changed, and cells were treated. In selected instances, cells were then exposed to LPS (100 ng/ml) for 6 h in the presence of absence of OPN (50 μM). Unstimulated cells served as controls. Data are presented mean ± SEM of four experiments (*, $p < 0.02$ LPS+siRNA OPN vs LPS, LPS+siRNA MM, and OPN+LPS+siRNA OPN).

iNOS and Tap1, was performed (12, 13). In selected instances, OPN expression was transiently ablated using siRNA (siRNA OPN) directed against OPN. A siRNA MM with limited homology to mouse genes served as the siRNA-negative control. As we and others (2, 12–14) have previously demonstrated, LPS induced iNOS, Tap1, and OPN protein expression in RAW264.7 cells. Ablation of OPN expression with siRNA in the presence of LPS was associated with a 6-fold increase iNOS and Tap1 protein in comparison to LPS alone ($p < 0.01$ LPS vs LPS+siRNA OPN). In addition, in the presence of siRNA, LPS induced OPN expression in both the cell lysate, and the culture medium were ablated. Addition of exogenous OPN (50 μM) to LPS+siRNA OPN cells restores iNOS and Tap1 to levels equivalent to those of LPS alone. These results indicate that inhibition of OPN expression is associated with significantly increased expression of iNOS and Tap1 protein.

Northern blot analysis was then performed to determine the role of OPN in regulation of iNOS and Tap1 steady-state mRNA levels (Fig. 2*b*). LPS was associated with induction of OPN, iNOS, and Tap1 mRNA. Ablation of OPN mRNA with siRNA was associated with a 10-fold increase in mRNA for both iNOS and Tap1 ($p < 0.01$ vs LPS). Addition of exogenous OPN (50 μM) to LPS+siRNA OPN cells restored iNOS and Tap1 mRNA to levels equivalent to those of LPS alone. In the setting of siRNA OPN alone, iNOS and Tap1 mRNA expression was not different from that of unstimulated controls (data not shown). These results indicate that inhibition of LPS-mediated OPN expression is associated with significantly increased iNOS and Tap1 mRNA expression. In total, this corroborates

our previously published findings that OPN inhibits iNOS protein and mRNA expression in the setting of LPS stimulation (2–4). In addition, OPN inhibits expression of another STAT1-dependent protein, Tap1.

OPN inhibits STAT1-dependent iNOS and Tap1 gene transcription

As differences in the steady-state levels of mRNA most commonly result from alterations in transcription, we performed a series of studies to determine the effect of OPN on iNOS and Tap1 gene transcription. To assess the effect of OPN on iNOS and OPN transcription, we measured the recruitment of RNA polymerase II to the iNOS and Tap1 promoter by ChIP assay (15) (Fig. 2*c*). Predictably, LPS stimulation increased both iNOS and Tap1 transcription over unstimulated controls. Ablation of OPN expression resulted in an additional 2- to 3-fold increase in iNOS and Tap1 transcription (*, $p < 0.01$ vs LPS). Repletion of OPN resulted in a level of iNOS and Tap1 transcription equivalent to that of LPS treatment alone. These results demonstrate that OPN inhibits iNOS and Tap1 gene transcription. The half-life of iNOS and Tap1 mRNA was measured by Northern blot analysis following actinomycin D (50 μg/ml) inhibition of global gene transcription. There was no difference in mRNA half-life detected between the LPS and LPS+siRNA OPN treatment groups for either iNOS or Tap1 (Fig. 2*e*). In the absence of actinomycin, there was no diminution of iNOS or Tap1 mRNA following LPS treatment.

Transient transfection analysis (Fig. 2*d*) was then performed to determine the role of OPN in transactivation of the iNOS and Tap1 promoters. In parallel with our previous findings, LPS stimulation results in significant transactivation of both the iNOS and Tap1 promoters. siRNA ablation of OPN in the presence of LPS results in a significant 4-fold increase in iNOS and Tap1 promoter activities (*, $p < 0.01$ vs LPS). Again, repletion of OPN restores promoter activities to levels equivalent to those seen with LPS treatment alone. Our findings indicate that OPN is associated with inhibition of maximal LPS-induced iNOS and Tap1 promoter activity.

Transcription and specifically, promoter activation, of individual genes are determined, in part, by DNA binding of transcriptional activators to specific regions of the promoter. Maximal activation of the iNOS promoter typically requires both NF-κB and STAT1 DNA binding (16). The murine iNOS promoter contains two NF-κB binding sites, NF-κB1 (nt −1044 to −1034) and NF-κB2 (nt −114 to −104) and a single STAT1 binding site (GAS; nt −942 to −934), deemed critical for iNOS expression (13, 17). Tap1 expression is known to be STAT1 dependent, and the Tap1 promoter contains proximal and distal GAS boxes: GAS1 (nt −172 to −163) and GAS2 (nt −247 to −240) (12). To delineate the effect of OPN on in vivo NF-κB and/or STAT1 DNA binding in the context of LPS-mediated iNOS and Tap1 promoter activation, ChIP/real-time PCR assays were performed (Fig. 3, *a* and *b*). In the iNOS promoter, LPS treatment significantly increased NF-κB binding to sites NF-κB1 and NF-κB2 while also increasing STAT1 bound to the GAS site (Fig. 3*a*). Manipulation of OPN expression did not alter NF-κB binding. In contrast, ablation of OPN expression significantly increased STAT1 bound by >4-fold ($p < 0.02$ LPS+siRNA OPN vs LPS). This finding was reversed when exogenous OPN was added to the LPS+siRNA OPN group. In a similar fashion, STAT1 binding to the Tap1 promoter at both of its GAS locations was increased significantly with LPS treatment. Knockdown of OPN with siRNA OPN increased STAT1 binding an additional 5-fold (*, $p < 0.01$ LPS+siRNA OPN vs LPS). Repletion with addition of exogenous OPN returned STAT1 binding to a level equivalent to that found with LPS treatment alone. These findings indicate that OPN expression in the context of LPS stimulation is associated with dramatically decreased STAT1 binding to the iNOS and Tap1 promoters in vivo. To further support a specific role for OPN in STAT1-dependent promoter transactivation, transient transfection assays were repeated using a pGL3 luciferase reporter plasmid construct bearing a quadruple repeat of the GAS enhancer element: agtttcataTTACTCTAAatc (Fig. 3*c*). LPS stimulation significantly increased STAT1-dependent luciferase activity in comparison to unstimulated controls. OPN knockdown in LPS+siRNA OPN results in an additional 3.5-fold increase in luciferase activity ($p < 0.02$ LPS+siRNA OPN vs LPS). This was ablated when OPN was returned to the system. Our results demonstrate that LPS-mediated OPN expression is associated with decreased STAT1 DNA binding and promoter transactivation, resulting in diminished iNOS and Tap1 gene transcription and protein expression.

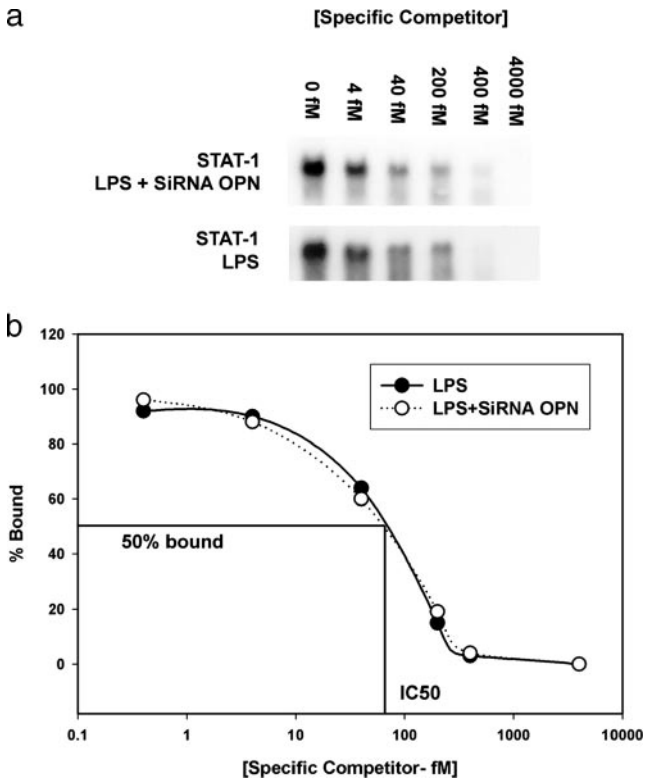

FIGURE 4. *a*, EMSAs of STAT1 binding. EMSAs were performed using nuclear extract from LPS- and LPS+siRNA OPN-treated cells and ^{32}P-labeled oligonucleotide (4.0 fM) bearing a single copy of the GAS consensus binding sequence. In specific competitor studies, gel shift assays were repeated with the addition of increasing concentrations (0.4–4000 fM) of unlabeled GAS oligonucleotide. Extent of STAT1 binding at each concentration of competitor was quantified by phosphorimaging; values in cpm were normalized to vary from 0 to 100% STAT1 binding. To adjust for the decreased signal strength in LPS cells, the specific activity of the target oligo was 2- to 3-fold greater for these cells vs the LPS+siRNA OPN cells. The gel is representative of three experiments. *b*, Competitive binding relationship for STAT1 and GAS oligonucleotide. A composite homologous competitive binding curve was constructed; Ki was calculated from the Cheng-Prusoff equation (18). The Ki for STAT1 from LPS- and LPS+siRNA OPN-treated cells were not statistically different, 66 ± 3 and 63 ± 4 fM, respectively.

OPN increases degradation of activated STAT1 protein

The potential mechanisms by which OPN may alter STAT1 DNA binding include: 1) decreased activation of STAT1 as reflected in

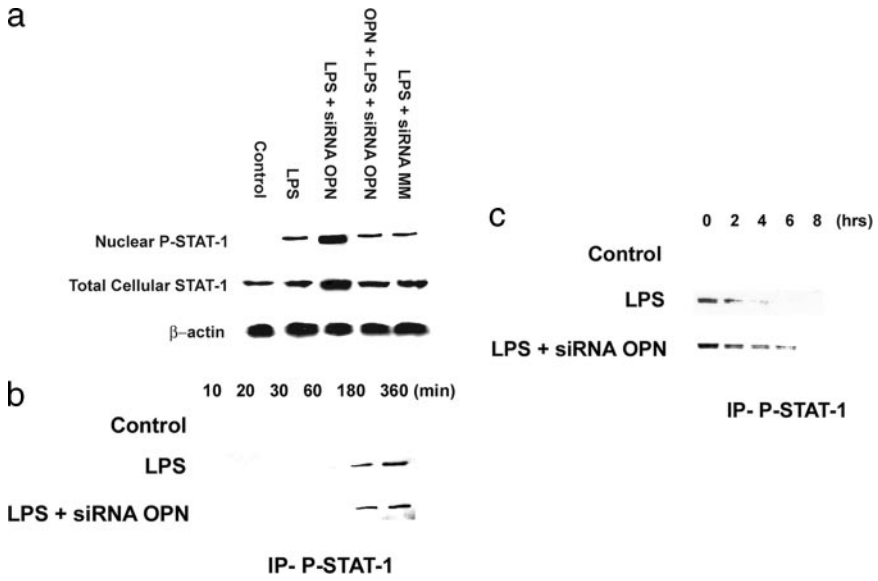

FIGURE 5. *a*, Immunoblot analysis of STAT-1 and P-STAT1 in cell lysate and nuclear fraction. Cells were transiently transfected with siRNA OPN or the mismatch control siRNA MM for 24 h. In selected instances, cells were then exposed to LPS (100 ng/ml) for 6 h in the presence of absence of OPN (50 μM). Unstimulated cells served as controls. Membranes were incubated with primary Ab to STAT1, P-STAT1, and β-actin followed by HRP-conjugated secondary Ab. The blot is representative of three experiments. *b*, Pulse and pulse-chase studies for STAT1 protein. Cells were transiently transfected with siRNA OPN or the mismatch control siRNA MM for 24 h. In selected instances, cells were then exposed to LPS (100 ng/ml) for 6 h. Unstimulated cells served as controls. The medium was then changed to one without methionine and cysteine. [^{35}S]Methionine/cysteine (100 μCi/ml) was added for the times indicated. For pulse-chase analysis, the protocol was altered to re-expose cells to complete medium with excess methionine (10 mM) and cysteine (3 mM) and allowed to incubate. Equal amounts of total protein were immunoprecipitated with STAT1 Ab. *b*, Pulse study for STAT1 protein. The blot is representative of three experiments. *c*, Pulse-chase study for STAT1 protein. The blot is representative of three experiments.

altered DNA binding affinity and/or 2) decreased amounts of activated STAT1 resulting from a) decreased synthesis and/or b) increased degradation.

To address the potential for OPN-dependent alteration in STAT1 DNA binding affinity, we constructed homologous competitive binding curves for STAT1 from LPS- and LPS+siRNA OPN-treated cells. EMSA were performed using nuclear extract (20 μg) from LPS- and LPS+siRNA OPN-treated cells and ^{32}P-labeled oligonucleotide (4.0 fM) bearing a single copy of the GAS consensus binding sequence. In specific competitor studies, gel shift assays were repeated with the addition of increasing concentrations (0.4–4000 fM) of unlabeled GAS oligonucleotide. A homologous competitive binding curve was then constructed; Ki was calculated from the Cheng-Prusoff equation, which simplifies to K_d = Ki = IC_{50} − (radiolabeled GAS oligo) (18). A representative gel shift experiment is depicted in Fig. 4*a*; the composite binding curve is shown in Fig. 4*b*. The Ki for STAT1 from LPS- and LPS+siRNA OPN-treated cells were not statistically different, 66 ± 3 and 63 ± 4 fM, respectively. The GAS oligonucleotide probe exhibits equal affinity for STAT1 from each of the two treatment settings. This result indicates that OPN does not alter DNA binding affinity of activated STAT1 for its consensus GAS binding site.

Activated STAT1 is phosphorylated at Tyr^{701}. STAT1 Tyr^{701} phosphorylation induces STAT1 dimerization, nuclear translocation, and DNA binding (19). To determine the potential impact of OPN on the total mass of cellular STAT1 and its activated form, nuclear phosphorylated Tyr^{701} STAT1 (P-STAT1), immunoblot analysis was performed on total cell protein and nuclear protein using Ab to STAT1 and P-STAT1 (Fig. 5*a*). Cells were treated for a period of 6 h before extraction of protein. P-STAT1 was readily detected following LPS treatment. Inhibition of OPN expression resulted in an 8-fold increase in both total cellular STAT1 and nuclear P-STAT1, as determined by densitometric analysis ($p < 0.05$ vs LPS alone). Repletion of OPN restored total STAT and P-STAT1 levels to that noted in LPS cells. When OPN alone is added to the system in the absence of LPS, STAT1 and P-STAT1 expression are unaltered in comparison to controls (data not shown). These data demonstrate that OPN decreases total STAT1 and nuclear P-STAT1 content in the setting of LPS exposure.

Next, we used pulse and pulse-chase studies to examine the effect of OPN on synthesis and/or degradation of P-STAT1 (Fig. 5, *b* and *c*). As depicted in Fig. 5*b*, the pulse experiments demonstrate no difference in P-STAT1 synthesis between LPS and LPS+siRNA OPN treatments conditions. In contrast, the pulse-chase experiments (Fig. 5*c*) indicate that inhibition of OPN expression in the presence of LPS is associated with increased duration of P-STAT1 protein expression. Following phosphorimaging analysis, a semilog plot of P-STAT1 protein (normalized to that of β-actin) vs time demonstrated that the P-STAT1 protein half-life in LPS cells was 1.5 ± 0.2 h compared with 3.6 ± 0.3 h in LPS+siRNA OPN cells ($p < 0.05$ LPS vs LPS+siRNA OPN). We conclude that OPN increases degradation of activated STAT1 protein in the setting of LPS stimulation.

OPN regulates STAT1 protein degradation by the Ub-proteasome pathway

As the Ub-proteasome system is a potential pathway by which STAT1 protein is degraded, we incubated RAW264.7 cells under various treatment conditions (as above) in the presence of cycloheximide (10 μg/ml) to inhibit protein synthesis. In selected instances, the 26S proteasome inhibitor, MG132 (10 μM) was also added. Cell lysates were assayed by immunoblotting for P-STAT1 (Fig. 6*a*). In the presence of LPS, minimal P-STAT1 was noted at all time points; MG132 significantly increased the amount and duration of detected P-STAT1 protein. In contrast, in LPS plus siRNA OPN, P-STAT1 levels were increased by >10-fold at all time points when compared with those of LPS alone; addition of MG132 did not significantly alter P-STAT1 expression. Finally,

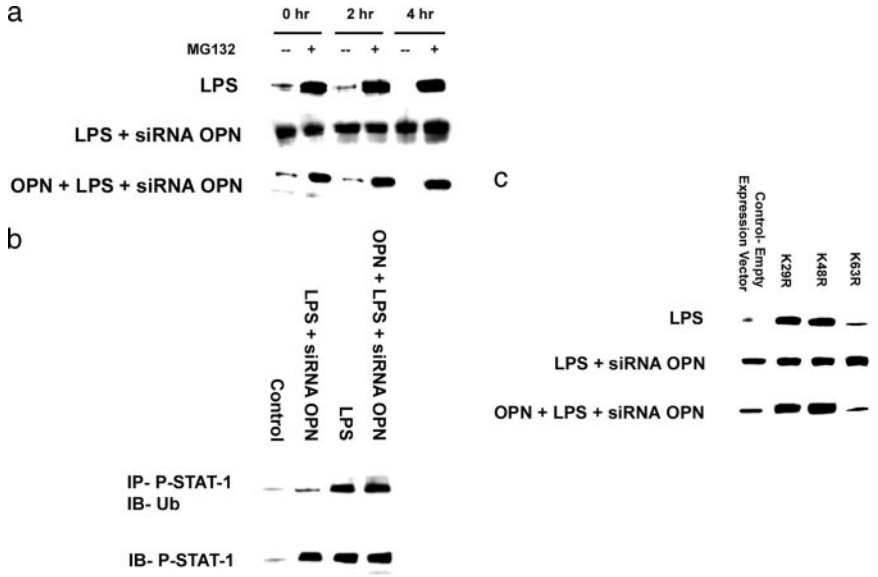

FIGURE 6. *a*, STAT1 degradation and the 26S proteosome. Cells were transiently transfected with siRNA OPN or the mismatch control siRNA MM for 24 h. In selected instances, cells were then exposed to LPS (100 ng/ml) for 6 h in the presence of absence of OPN (50 μM). Unstimulated cells served as controls. All cells were treated with cycloheximide to inhibit protein synthesis. In selected instances, the 26S proteasome inhibitor, MG132 (10 μM), was also added. Cell lysates were assayed by immunoblotting for P-STAT1. The blot is representative of three experiments. *b*, OPN and ubiquitination of P-STAT1. Coimmunoprecipitation studies were performed to assess the extent of ubiquitination-associated P-STAT1. Cells were transiently transfected with siRNA OPN. Unstimulated cells served as controls. In selected instances, cells were then exposed to LPS (100 ng/ml) for 6 h in the presence or absence of OPN (50 μM). Cycloheximide (10 μg/ml) was added for 30 min, and the cells were incubated with fresh medium in the presence of MG132 (10 μM). Cell lysates (500 μg) were immunoprecipitated with P-STAT1 Ab and immunoblotted with anti-Ub Ab. The blot is representative of four experiments. *c*, Ubiquitination of P-STAT1 is necessary for its degradation. Ub mutant K48R, K29R, and K63R expression vectors were constructed and used in treated RAW cells. Cycloheximide (10 μg/ml) was added, and the cells were incubated with fresh medium in the presence of MG132 (10 μM). Immunoblot analysis was then performed for P-STAT1. The blot is representative of three experiments.

repletion of OPN to this setting restored the expression pattern of P-STAT1 to a level similar to that of LPS treatment alone. Inhibitors of calpains (5 μM calpastatin) and lysosomal enzymes (50 μM leupeptin) had no effect on P-STAT1 degradation in the context of LPS treatment. β-Actin protein levels were not altered (data not shown). In the setting of LPS stimulation, these data demonstrate that P-STAT1 levels are increased when proteasome activity is ablated and that inhibition of OPN expression is associated with increased P-STAT1 levels. These results indicate that the 26S proteasome degrades P-STAT1 protein levels in the presence of LPS-mediated OPN expression.

Coimmunoprecipitation studies were performed to assess the extent of ubiquitination-associated P-STAT1 under our various treatment conditions (8) (Fig. 6*b*). In the setting of LPS stimulation, there is an incremental 20-fold increase in P-STAT1 and P-STAT1 ubiquitination over that of unstimulated controls. However, when OPN expression is ablated in the LPS+siRNA OPN group, the extent of ubiquitination is decreased significantly by >16-fold ($p < 0.01$ vs LPS). Restoration of OPN to this treatment condition results in a dramatic increase in ubiquitinated P-STAT1 to a level no different from that of LPS. Immunoblot analysis for P-STAT1 was performed as a control. In the three settings with LPS, P-STAT1 levels were significantly greater than control. When Ub-P-STAT1 is considered relative to total P-STAT1, inhibition of OPN expression in LPS+ siRNA OPN is associated with significantly less Ub-P-STAT-1. These results indicate that LPS-associated OPN expression increases P-STAT1 ubiquitination.

However, ubiquitination alone does not allow us to conclude that P-STAT1 is degraded by the Ub-proteasome pathway. Although Ub Lys^{48} is the primary site of isopeptide polyubiquitination required to target proteins for degradation, polyubiquitin chains linked through Lys^{29} also target proteins for degradation. In contrast, Ub Lys^{63} is involved in endosomal trafficking and in activation of TLR pathways. K48R and K29R Ub mutants act as Ub dominant negatives (DN), resulting in premature termination of Ub chains and inhibition of degradation by the proteasome. K63R Ub mutants do not alter proteasome dependent protein degradation (20). To confirm that ubiquitination is required for degradation of P-STAT1 in LPS-treated RAW cells, we constructed Ub mutant K48R, K29R, and K63R expression vectors and used these in treated RAW cells. Immunoblot analysis was then performed for P-STAT1 (Fig. 6*c*). Transfection of K48R or K29R Ub mutants resulted in higher levels of P-STAT1 in the presence of LPS stimulation; this is in keeping their role as DN inhibitors of Ub-mediated proteasome degradation. When OPN expression was knocked down in this setting, P-STAT1 levels were elevated in the control setting and did not change in the presence of the Ub DN expression vectors. Return of OPN to the system resulted in a P-STAT1 profile similar to that of LPS alone. K63R did not alter the pattern of P-STAT1 levels under any treatment condition. There was no change of glyceraldehyde-3-phosphate dehydrogenase, which is degraded by the lysosomal pathway (data not shown). These data confirm that: 1) ubiquitination of P-STAT1 is required for degradation, and 2) inhibition of OPN expression decreases Ub-associated P-STAT1 degradation.

OPN mediates STAT1 degradation and regulates STAT1 dependent gene transcription in BMM

To determine the in vivo role of OPN in STAT1 degradation and STAT1-dependent gene transcription, additional studies were performed in primary murine bone marrow-derived macrophages. Cells were a gift from Dr. Y. He (Duke University). Immunoblot analysis was performed for P-STAT1 (Fig. 7*a*). The data demonstrate that P-STAT1 levels are induced in the presence of LPS and

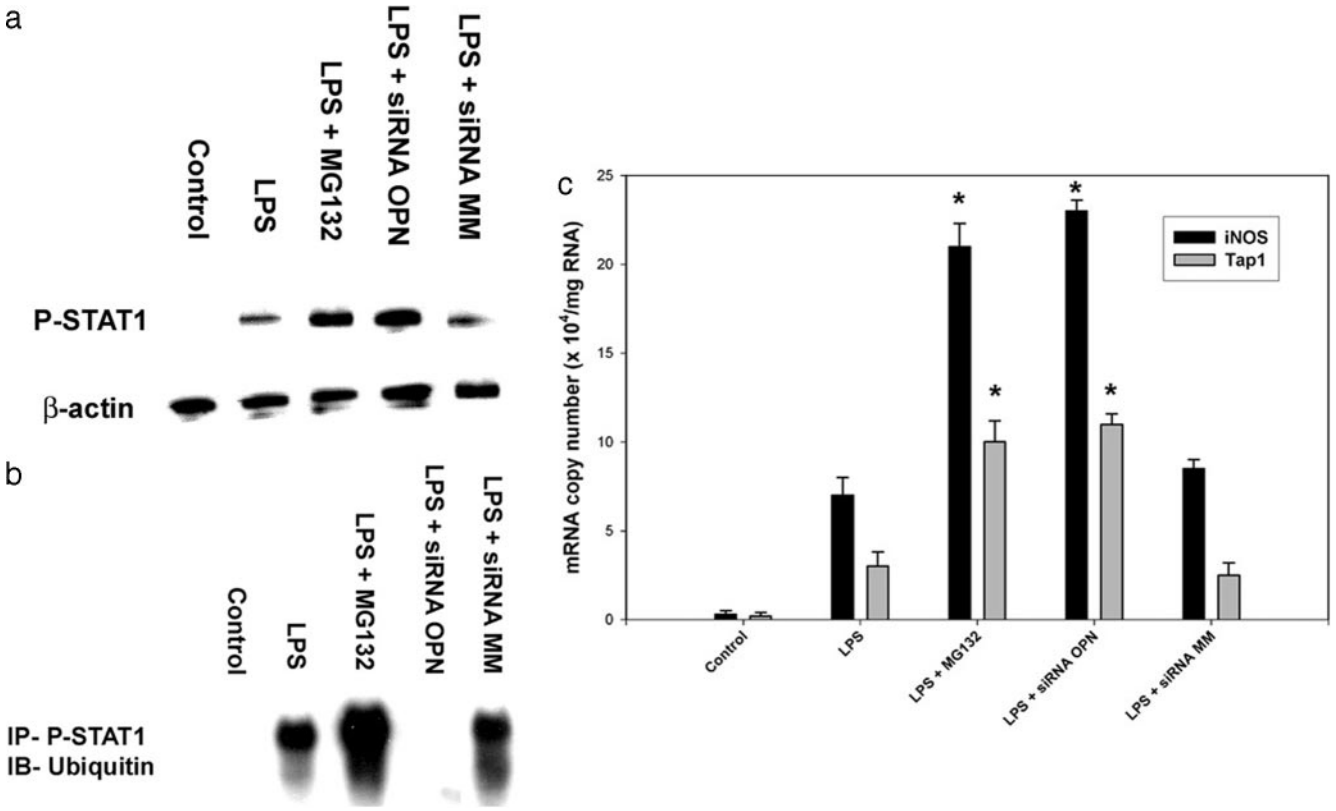

FIGURE 7. *a*, OPN and P-STAT1 protein expression in murine BMM in primary culture. Cells were transiently transfected with siRNA OPN or the mismatch control siRNA MM for 24 h. In selected instances, cells were then exposed to LPS (100 ng/ml) for 6 h in the presence of absence of MG132 (10 μM). Unstimulated cells served as controls. Cell lysate was separated by SDS-PAGE and electrotransferred. Membranes were incubated with primary Ab to P-STAT1 and β-actin, followed by HRP-conjugated secondary Ab. The blot is representative of three experiments. *b*, Ubiquitination of P-STAT1 in BMM. Cells were transiently transfected with siRNA OPN or the mismatch control siRNA MM for 24 h. In selected instances, cells were then exposed to LPS (100 ng/ml) for 6 h in the presence of absence of MG132 (10 μM). Unstimulated cells served as controls. Cell lysates (500 μg) were immunoprecipitated with P-STAT1 Ab and immunoblotted with anti-Ub Ab. The blot is representative of four experiments. *c*, Tap1 and iNOS mRNA expression in BMM. Cells were transiently transfected with siRNA OPN or the mismatch control siRNA MM for 24 h. In selected instances, cells were then exposed to LPS (100 ng/ml) for 6 h in the presence of absence of MG132 (10 μM). Unstimulated cells served as controls. Quantitative RT-PCR was conducted. The amount of each mRNA (iNOS and Tap1) was normalized to β-actin. Data are presented mean ± SEM of four experiments (*, $p < 0.02$ LPS+siRNA OPN and LPS+MG132 vs LPS and LPS+siRNA MM for iNOS and Tap1).

subsequently significantly increased by ~7-fold in the presence of the proteasome inhibitor, MG132, and/or siRNA inhibition of OPN expression. To further confirm our earlier findings in this primary murine macrophage system, we then performed IP for P-STAT1, and immunoblots were repeated using Ab to Ub to determine Ub-STAT1 expression (Fig. 7*b*). As expected, LPS induces a Ub-P-STAT1 smear that is significantly increased with the addition of MG132. In the absence of OPN as mediated by siRNA OPN, LPS does not induce formation of Ub-P-STAT1. In LPS-treated primary murine macrophages, these data indicate that OPN is required for ubiquitination of P-STAT1 and that inhibition of 26S proteasome function impairs P-STAT1 degradation.

As a correlative study, Q-PCR was performed in these primary cultured macrophages under the same treatment conditions to determine the effect of LPS and OPN on steady-state mRNA levels of the STAT-1-dependent genes, iNOS and Tap1 (Fig. 7*c*). LPS-induced expression of the STAT-dependent genes, iNOS and Tap1, is significantly increased in the presence of MG132 or inhibition of OPN expression when compared with those of unstimulated controls and LPS alone ($p < 0.02$ LPS+MG132 or LPS+siRNA OPN vs LPS or control). These data indicate that OPN expression decreases steady-state levels of iNOS and Tap1 mRNA in the setting of LPS stimulation. In combination with our previous results in Fig. 7, *a* and *b*, these results indicate that LPS associated OPN expression: 1) mediates STAT1 degradation via the Ub-26S proteasome system in primary murine macrophages, and 2) inhibits maximal expression of STAT1-dependent genes, iNOS and Tap1.

SLIM protein and STAT1 degradation

Ubiquitination plays a major role in regulating many cellular processes by marking proteins, including transcription factors, for degradation through the 26s proteasome-dependent pathway (21). Conjugation of Ub to target proteins requires three enzymes, Ub-activating enzyme (E1), Ub-conjugating enzyme (E2), and E3. E3 interacts with both E2 and the target protein to facilitate transfer of Ub to the substrate. It is E3 ligase that confers specificity to the reaction. In the case of STAT1, Kim and Maniatis (8) were the first to demonstrate that IFN-activated STAT1 levels may be regulated by the Ub-proteasome pathway. In 2005, Tanaka et al. (10) were identified SLIM protein as a STAT Ub E3 ligase and demonstrated a central role for ubiquitination in regulation of the IFN-STAT signaling pathway. We investigated the potential contribution of SLIM as the Ub E3 ligase in our system of OPN-mediated STAT1 degradation. First, we sought to confirm interaction by ectopic co-expression of Flag-STAT1 and His-SLIM in COS-1 cells and subsequent immunoprecipitation of STAT1 following treatment (Fig. 8*a*). The resulting coimmunoprecipitation of STAT1 with SLIM

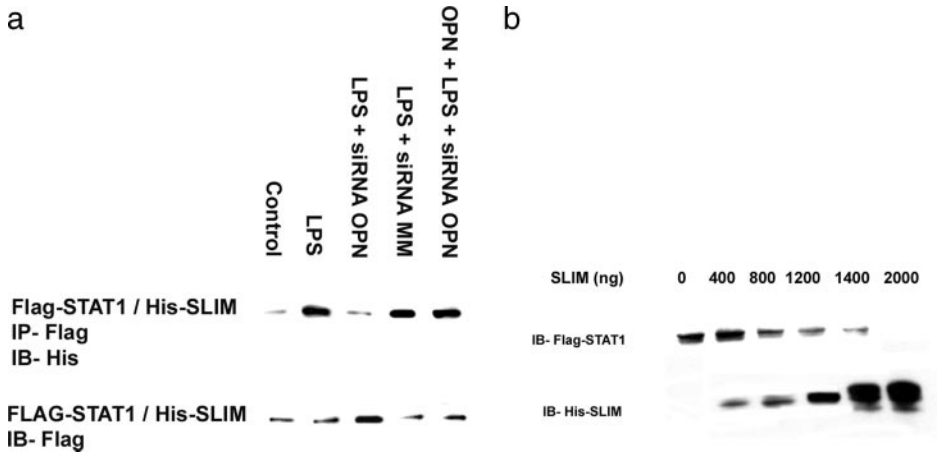

FIGURE 8. *a*, SLIM and STAT1 association. Flag-STAT1 and His-SLIM in COS-1 cells were ectopically expressed in COS-1 cells. Cells were transiently transfected with siRNA OPN or the mismatch control siRNA MM for 24 h. In selected instances, cells were then exposed to LPS (100 ng/ml) for 6 h in the presence of absence of OPN (50 μM). Unstimulated cells served as controls. Subsequently, STAT1 immunoprecipitation was performed followed by immunoblotting for SLIM. The blot is representative of three experiments. *b*, SLIM induces STAT1 degradation. COS-1 cells were transfected with a constant amount of Flag-STAT1 in the absence or presence of increasing amounts of His-SLIM. COS-1 cells were then exposed to LPS (100 ng/ml) for a period of 6 h. Immunoblot analysis was then performed for STAT1 and SLIM. The blot is representative of three experiments.

suggests a mechanism by which STAT1 may undergo degradation. Next, we determined whether SLIM could induce STAT1 degradation. By cotransfecting LPS-treated COS-1 cells with a constant amount of Flag-STAT1 in the absence or presence of increasing amounts of His-SLIM, we found that SLIM was, in a dose-dependent manner, able to induce the degradation of STAT1 in the presence of LPS (Fig. 8*b*). In the absence of LPS treatment, there was no change in levels of FLAG-STAT1 despite increasing amounts of transfected SLIM (data not shown). As our initial results clearly show a role for SLIM in mediating the degradation of STAT1, we examined whether endogenous STAT1 could undergo in SLIM$^{-/-}$ MEF cells (Fig. 9*a*). Wild-type and SLIM$^{-/-}$ MEF were transfected with Flag-STAT1, HA-Ub, and/or His-tagged OPN vectors. Following incubation in the presence of LPS and MG132, immunoprecipitation was performed using M2 anti-Flag and immunoblots probed with Ab to HA. There are minimal amounts of Ub-STAT1 in the SLIM$^{-/-}$ MEF. In contrast, there is significantly greater amounts of Ub-STAT1 in the wild-type MEF. In this context, addition of the His-OPN expression vector to the wild-type MEF system is associated with significantly greater Ub-STAT1. Taken together, these studies using SLIM overexpression and deficiency demonstrate a direct role for OPN and SLIM in mediating STAT1 ubiquitination and degradation.

In the following set of studies, we return to our RAW264.7 macrophage model to determine whether the SLIM polyubiquitinates STAT1 in the presence of LPS and OPN. We incubated the cells under various treatment conditions in the presence and absence of siRNA SLIM and analyzed total cell lysates by immunoblotting for P-STAT1 (Fig. 9*b*). Immunoblot analysis demonstrates that OPN was expressed was cells were exposed to LPS. SLIM is readily detected in both wild-type and siRNA MM-treated cells under control and LPS treatment conditions. In these cells, minimal P-STAT1 was noted under LPS treatment. In the siRNA SLIM cells, no SLIM was found, but a significantly greater level P-STAT1 was detected under LPS treatment despite the presence of OPN. When LPS is combined with MG132, levels of P-STAT1 in wild-type and siRNA MM are increased to levels equivalent to that noted in si-RNA-SLIM cells. These results suggest that SLIM is required for proteasome-dependent STAT1 degradation in LPS-treated RAW264.7 cells.

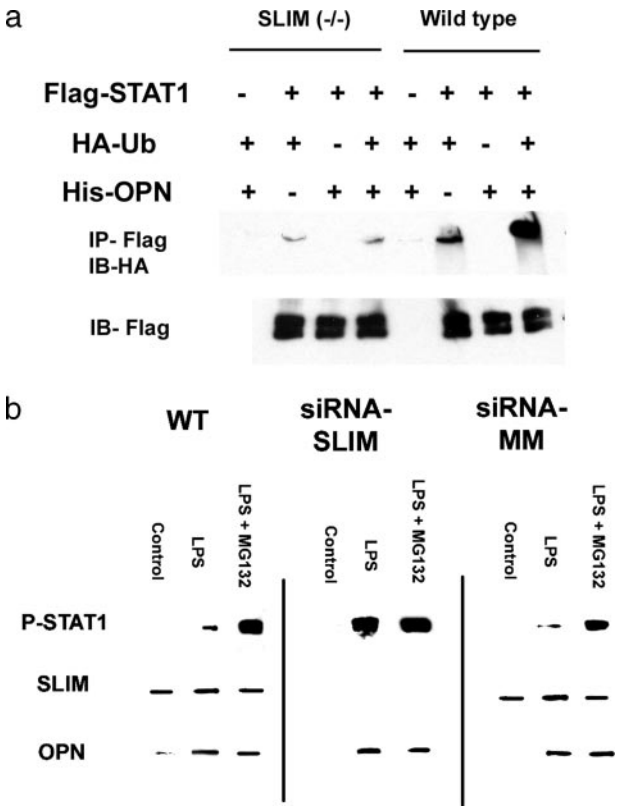

FIGURE 9. *a*, STAT1 expression in wild-type and SLIM$^{-/-}$ MEF. Wild-type and SLIM$^{-/-}$ MEF were transfected with Flag-STAT1, HA-Ub, and/or His-tagged OPN vectors. Following incubation in the presence of LPS (100 ng/ml) and MG132 (10 μM), immunoprecipitation of STAT1 was performed using M2 anti-Flag and immunoblots for Ub and STAT1 performed with Ab to HA and Flag. The blot is representative of three experiments. *b*, SLIM and STAT1 in LPS-treated RAW264.7 murine macrophages. Cells were transiently transfected with siRNA SLIM or the mismatch control siRNA MM for 24 h. In selected instances, cells were then exposed to LPS (100 ng/ml) for 6 h in the presence of absence of MG132 (10 μM). Unstimulated cells served as controls. Total cell lysates were analyzed by immunoblotting for P-STAT1, SLIM, and OPN. The blot is representative of three experiments.

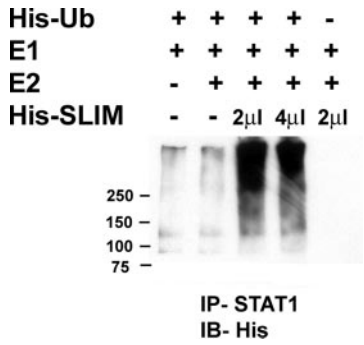

FIGURE 10. SLIM and in vitro ubiquitination assay. Recombinant His-tagged SLIM or empty His vector was expressed in COS-1 cells and purified to use as the source of E3 ligase. FLAG-tagged STAT1 was expressed in RAW264.7 cells and used as the source of substrate for in vitro ubiquitination. After in vitro ubiquitination, all samples were resolved by SDS-PAGE and transferred electrophoretically to PVDF membrane. STAT1 ubiquitination was detected by mouse anti-HisG Ab to determine Ub ladder formation. The blot is representative of three experiments.

Finally, to examine the possibility that SLIM is the Ub E3 ligase in this system and not simply a cofactor, we performed an in vitro ubiquitination assay (Fig. 10). In the presence of E1, E2, and Ub, recombinant SLIM was found to mediate the in vitro ubiquitination of STAT1 that was immunoprecipitated form LPS-treated RAW264.7 macrophages. In the presence of empty His vector, no ubiquitinated STAT1 was found. In total, using a system of LPS-treated RAW264.7 murine macrophages, these results demonstrate that OPN-mediated STAT1 degradation by the Ub proteasome pathway requires SLIM as the E3 ligase.

Discussion

In endotoxin-mediated sepsis and septic shock, proinflammatory cytokines are elaborated, and iNOS is systemically expressed in multiple cell types, including macrophages (14). The sustained production of NO in high concentration regulates multiple cellular and biochemical functions, including inotropic and chronotropic cardiac responses, systemic vasomotor tone, intestinal epithelial permeability, endothelial activation, and microvascular permeability (1). The cellular and biochemical consequences of NO production in the setting of sepsis are exemplified by DNA single-strand breakage, ADP ribosylation of nuclear proteins, nitrosative stress-mediated alteration in gene transcription, and inhibition of mitochondrial respiration. In experimental endotoxemia, NO production results in cytotoxicity, inhibition of mitochondrial respiration, platelet aggregation, neutrophil adhesion, hypotension, and vasoplegia (22, 23). However, evidence indicates that LPS-mediated iNOS gene transcription is an exceedingly complex and redundant signal transduction pathway with varying signal- and cell-dependent responses. Specifically, in systemic inflammation induced by LPS, the macrophage is responsible for the majority of the circulating NO metabolites. Macrophage iNOS expression is central to many of the systemic effects associated with LPS stimulation. However, while the molecular pathways that up-regulate iNOS expression have been studied extensively in multiple cell types, including the macrophage, little is known of the parallel counter-regulatory pathways that repress or inhibit macrophage iNOS expression in the context of endotoxemia and sepsis. In this study, using a system of LPS-treated RAW264.7 macrophages, we demonstrate that OPN regulates Ub-dependent degradation of STAT1 through the activity of SLIM as the Ub E3 ligase. This regulation of STAT1 degradation underlies OPN′s effect as an inhibitor of iNOS gene transcription. These are novel findings and define OPN as a unique and as yet, poorly characterized, transactivator of STAT1 degradation by the Ub-proteasome system.

STAT signaling is tightly regulated and several mechanisms have been proposed to account for this control (24). The suppressor of cytokine signaling (SOCS) and protein inhibitor of STAT (PIAS) families of proteins have been shown to bind to and inhibit either the cytokine receptor-associated JAK or activated STAT molecule, respectively. SOCS proteins are induced following cytokine stimulation, bind to JAK kinases, and inhibit activated JAK kinases from further phosphorylation of STAT proteins (25, 26). As a result of inhibition by SOCS proteins, STAT signaling becomes a transient response, and levels of phosphorylated STAT proteins decrease within hours of activation. However, the SOCS feedback mechanism does not result in reduced levels of STAT proteins. Each member of the PIAS family has been shown to inhibit STAT-mediated gene activation. Another mechanism known to down-regulate STAT signaling involves tyrosine phosphatases, such as Src homology region 2 domain-containing phosphatases 1 and 2. These tyrosine phosphatases have been shown to down-regulate the activity of STAT1, STAT3, or STAT5 following activation by IFN-γ, leukemia inhibitory factor, or IL-2 either by dephosphorylating STAT proteins directly or through dephosphorylation of JAK kinases (27–29). Like the SOCS feedback and PIAS mechanisms, the down-regulation through tyrosine phosphatases also does not lead to reduced levels of STAT proteins. Other posttranslational modifications of STAT proteins, such as arginine methylation, acetylation, and ubiquitination, have been suggested as important means to regulate STAT signaling. Polyubiquitination of substrates targets them for degradation by the 26S proteasome. E3 Ub ligases confer specificity to the ubiquitination reaction. The E3 ligase transfers Ub from the E2 enzyme to a lysine residue on a substrate protein, resulting in an isopeptide bond between the substrate lysine and the C terminus of Ub. Ub ligation provides the key step of substrate selection and Ub transfer to the protein target. There are at least four classes of E3 ligases: HECT type, RING type, PHD type, and U-box containing. For a specific substrate, E3 ligase is the only member of the E1, E2, and E3 sequence that undergoes regulation (30, 31). SLIM contains a PDZ domain and a LIM domain and interacts in the nucleus with tyrosine phosphorylated STAT molecules (32). The LIM domain forms a zinc-finger structure related to the RING finger and PHD structures; similar proteins have been shown to possess E3 ligase activity (32). SLIM inhibits gene expression mediated by STAT4 or STAT1 by promoting ubiquitination and degradation of STAT4 and STAT1. The cDNA encoding mouse SLIM is 1509 bp (GenBank accession no. BC024556) for mouse with an open reading frame of 349 aa (10, 32). It is expressed as a 38-kDa nuclear protein. The human transcript (GenBank accession no. NM_021630) is homologous to mouse with 77% identity at the amino acid level and 79% identical at the cDNA level. It is highly expressed in lung, spleen, thymocytes, and primary hemopoietic cells, including macrophages. SLIM is the first identified Ub ligase with specificity for STAT proteins.

The signal transduction pathway that links OPN and SLIM is unknown. There are two possibilities. In the first, OPN may induce expression of SLIM, which is constitutively active. A second and more likely possibility is that OPN may simply activate constitutively expressed SLIM via a posttranslational mechanism. Given our results in Fig. 9*b*, it appears that SLIM is indeed constitutively expressed and that OPN may therefore activate SLIM via posttranslational modification. As OPN is a secreted protein that binds to both cell surface $\alpha_v\beta_3$ integrins bearing a RGD binding motif and/or CD44, future studies delineating the OPN-SLIM relationships may begin at the level of OPN′s cell surface receptors.

OPN is a secreted glycoprotein that is rich in aspartate and sialic-acid residues and contains functional domains for calcium-binding, phosphorylation, glycosylation, and extracellular matrix adhesion (33). OPN appears to mediate cell-matrix interactions and cellular signaling through binding with integrin, primarily $\alpha_v\beta_3$, and CD44 receptors. OPN is expressed in multiple species, including humans and rodents (34). Cells that express OPN include osteoclasts, osteoblasts, kidney, breast and skin epithelial cells, nerve cells, vascular smooth muscle cells, and endothelial cells (33, 35–38). Activated immune cells such as T cells, NK cells, macrophages, and Kupffer cells also express OPN. The secreted OPN protein is widely distributed in plasma, urine, milk, and bile (39–41). Constitutive expression of OPN exists in several cell types but induced expression is detected in T lymphocytes, epidermal cells, bone cells, macrophages, and tumor cells in remodeling processes such as inflammation, ischemia-reperfusion, bone resorption, and tumor progression (33, 37, 38). A variety of stimuli, including PMA, 1,25-dihydroxyvitamin D, basic fibroblast growth factor, TNF-α, IL-1, IFN-γ, and LPS, appears to up-regulate OPN expression (33, 37, 38, 42). OPN has multiple molecular functions that mediate cell adhesion, chemotaxis, macrophage-directed IL-10 suppression, stress-dependent angiogenesis, prevention of apoptosis, and anchorage-independent growth of tumor cells (33, 37, 38, 42). With regard to our findings, we define OPN to be a unique and as yet, poorly characterized, transactivator of STAT1 degradation by the Ub-proteasome system in LPS treated macrophages.

Disclosures

The authors have no financial conflict of interest.

References

1. Doursout, M. F., R. G. Kilbourn, C. J. Hartley, and J. E. Chelly. 2000. Effects of *N*-methyl-L-arginine on cardiac and regional blood flow in a dog endotoxin shock model. *J. Crit. Care* 15: 22–29.
2. Guo, H., C. Q. Cai, R. A. Schroeder, and P. C. Kuo. 2001. Osteopontin is a negative feedback regulator of nitric oxide synthesis in murine macrophages. *J. Immunol.* 166: 1079–1086.
3. Gao, C., H. Guo, J. Wei, Z. Mi, P. Wai, and P. C. Kuo. 2004. *S*-nitrosylation of hnRNP-A/B regulates osteopontin transcription in endotoxin-stimulated murine macrophages. *J. Biol. Chem.* 279: 11236–11243.
4. Gao, C., H. Guo, J. Wei, Z. Mi, P. Wai, and P. C. Kuo. 2004. *S*-nitrosylation of heterogeneous nuclear ribonucleoprotein A/B regulates osteopontin transcription in endotoxin-stimulated murine macrophages. *J. Biol. Chem.* 279: 11236–11243.
5. Galea, E., D. J. Reis, E. S. Fox, H. Xu, and D. L. Feinstein. 1996. CD14 mediates endotoxin induction of nitric oxide synthase in cultured brain glial cells. *J. Neuroimmunol.* 64: 19–28.
6. Meraz, M. A., J. M. White, K. C. Sheehan, E. A. Bach, S. J. Rodig, A. S. Dighe, D. H. Kaplan, J. K. Riley, A. C. Greenlund, D. Campbell, et al. 1996. Targeted disruption of the *Stat1* gene in mice reveals unexpected physiologic specificity in the JAK-STAT signaling pathway. *Cell* 84: 431–442.
7. Nishiya, T., T. Uehara, H. Edamatsu, Y. Kaziro, H. Itoh, and Y. Nomura. 1997. Activation of Stat1 and subsequent transcription of inducible nitric oxide synthase gene in C6 glioma cells is independent of interferon γ-induced MAPK activation that is mediated by p21ras. *FEBS Lett.* 408: 33–38.
8. Kim, T. K., and T. Maniatis. 1996. Regulation of interferon γ-activated STAT1 by the ubiquitin-proteasome pathway. *Science* 273: 1717–1719.
9. Mowen, K. A., J. Tang, W. Zhu, B. T. Schurter, K. Shuai, H. R. Herschman, and M. David. 2001. Arginine methylation of STAT1 modulates IFNα/β-induced transcription. *Cell* 104: 731–741.
10. Tanaka, T., M. A. Soriano, and M. J. Grusby. 2005. SLIM is a nuclear ubiquitin E3 ligase that negatively regulates STAT signaling. *Immunity* 22: 729–736.
11. Wai, P. Y., Z. Mi, H. Guo, S. Sarraf-Yazdi, C. Gao, J. Wei, C. E. Marroquin, B. Clary, and P. C. Kuo. 2005. Osteopontin silencing by small interfering RNA suppresses in vitro and in vivo CT26 murine colon adenocarcinoma metastasis. *Carcinogenesis* 26: 741–751.
12. Marques, L., M. Brucet, J. Lloberas, and A. Celada. 2004. STAT1 regulates lipopolysaccharide- and TNF-α-dependent expression of transporter associated with antigen processing 1 and low molecular mass polypeptide 2 genes in macrophages by distinct mechanisms. *J. Immunol.* 173: 1103–1110.
13. Gao, J., D. C. Morrison, T. J. Parmely, S. W. Russell, and W. J. Murphy. 1997. An interferon γ-activated site (GAS) is necessary for full expression of the mouse iNOS gene in response to interferon γ and lipopolysaccharide. *J. Biol. Chem.* 272: 1226–1230.
14. Xie, Q. W., and C. Nathan. 1994. The high output nitric oxide pathway: role and regulation. *J. Leukocyte Biol.* 56: 576–582.
15. Setiadi, A. F., M. D. David, S. S. Chen, J. Hiscott, and W. A. Jefferies. 2005. Identification of mechanisms underlying transporter associated with antigen processing deficiency in metastatic murine carcinomas. *Cancer Res.* 65: 7485–7492.
16. Xie, Q. W., R. Whisnant, and C. Nathan. 1993. Promoter of the mouse gene encoding calcium independent nitric oxide synthase confers inducibility by interferon γ and bacterial lipopolysaccharide. *J. Exp. Med.* 177: 1779–1784.
17. Wei, J., H. Guo, C. Gao, and P. C. Kuo. 2004. Peroxide-mediated chromatin remodelling of a nuclear factor κB site in the mouse inducible nitric oxide synthase promoter. *Biochem. J.* 377: 809–818.
18. Cheng, Y., and W. H. Prusoff. 1973. Relationship between the inhibition constant (K1) and the concentration of inhibitor which causes 50 percent inhibition (I50) of an enzymatic reaction. *Biochem. Pharmacol.* 22: 3099–3108.
19. Stoiber, D., P. Kovarik, S. Cohney, J. A. Johnston, P. Steinlein, and T. Decker. 1999. Lipopolysaccharide induces in macrophages the synthesis of the suppressor of cytokine signaling 3 and suppresses signal transduction in response to the activating factor IFN-γ. *J. Immunol.* 163: 2640–2647.
20. Xiong, H., H. Li, H. J. Kong, Y. Chen, J. Zhao, S. Xiong, B. Huang, H. Gu, L. Mayer, K. Ozato, and J. C. Unkeless. 2005. Ubiquitin-dependent degradation of interferon regulatory factor-8 mediated by Cbl down-regulates interleukin-12 expression. *J. Biol. Chem.* 280: 23531–23539.
21. Liu, Y. C. 2004. Ubiquitin ligases and the immune response. *Annu. Rev. Immunol.* 22: 81–127.
22. Matthews, J. R., C. H. Botting, M. Panico, H. R. Morris, and R. T. Hay. 1996. Inhibition of NF-κB binding by nitric oxide. *Nucleic Acids Res.* 24: 2236–2242.
23. Brendelford, E. M., K. B. Andersson, and O. S. Gabrielsen. 1998. Nitric oxide disrupts specific DNA binding of the transcription factor c-Myb in vitro. *FEBS Lett.* 425: 52–56.
24. Shuai, K., and B. Liu. 2003. Regulation of JAK-STAT signalling in the immune system. *Nat. Rev. Immunol.* 3: 900–911.
25. Endo, T. A., M. Masuhara, M. Yokouchi, R. Suzuki, H. Sakamoto, K. Mitsui, A. Matsumoto, S. Tanimura, M. Ohtsubo, H. Misawa, et al. 1997. A new protein containing an SH2 domain that inhibits JAK kinases. *Nature* 387: 921–924.
26. Starr, R., T. A. Willson, E. M. Viney, L. J. Murray, J. R. Rayner, B. J. Jenkins, T. J. Gonda, W. S. Alexander, D. Metcalf, N. A. Nicola, and D. J. Hilton. 1997. A family of cytokine-inducible inhibitors of signalling. *Nature* 387: 917–921.
27. Haque, S. J., P. Harbor, M. Tabrizi, T. Yi, and B. R. Williams. 1998. Protein-tyrosine phosphatase Shp-1 is a negative regulator of IL-4- and IL-13-dependent signal transduction. *J. Biol. Chem.* 273: 33893–33896.
28. You, M., D. H. Yu, and G. S. Feng. 1999. Shp-2 tyrosine phosphatase functions as a negative regulator of the interferon-stimulated Jak/STAT pathway. *Mol. Cell. Biol.* 19: 2416–2424.
29. Bousquet, C., C. Susini, and S. Melmed. 1999. Inhibitory roles for SHP-1 and SOCS-3 following pituitary proopiomelanocortin induction by leukemia inhibitory factor. *J. Clin. Invest.* 104: 1277–1285.
30. Ungureanu, D., and O. Silvennoinen. 2005. SLIM trims STATs: ubiquitin E3 ligases provide insights for specificity in the regulation of cytokine signaling. *Sci. STKE* 2005: pe49.
31. Mansell, A., R. Smith, S. L. Doyle, P. Gray, J. E. Fenner, P. J. Crack, S. E. Nicholson, D. J. Hilton, L. A. O'Neill, and P. J. Hertzog. 2006. Suppressor of cytokine signaling 1 negatively regulates Toll-like receptor signaling by mediating Mal degradation. *Nat. Immunol.* 7: 148–155.
32. Loughran, G., N. C. Healy, P. A. Kiely, M. Huigsloot, N. L. Kedersha, and R. O'Connor. 2005. Mystique is a new insulin-like growth factor-I-regulated PDZ-LIM domain protein that promotes cell attachment and migration and suppresses Anchorage-independent growth. *Mol. Biol. Cell* 16: 1811–1822.
33. Denhardt, D. T., M. Noda, A. W. O'Regan, D. Pavlin, and J. S. Berman. Osteopontin as a means to cope with environmental insults: regulation of inflammation, tissue remodeling, and cell survival. *J. Clin. Invest.* 107: 1055–1061.
34. Attur, M. G., M. N. Dave, S. Stuchin, A. J. Kowalski, G. Steiner, S. B. Abramson, D. T. Denhardt, and A. R. Amin. Osteopontin: an intrinsic inhibitor of inflammation in cartilage. *Arthritis Rheum.* 44: 578–584.
35. Craig, A. M., and D. T. Denhardt. 1991. The murine gene encoding secreted phosphoprotein 1 (osteopontin): promoter structure, activity, and induction in vivo by estrogen and progesterone. *Gene* 100: 163–171.
36. Denhardt, D. T., and X. J. Guo. 1993. Osteopontin: a protein with diverse functions. *FASEB J.* 7: 1475–1482.
37. O'Regan, A., and J. S. Berman. 2000. Osteopontin: a key cytokine in cell-mediated and granulomatous inflammation. *Int. J. Exp. Pathol.* 81: 373–390.
38. Weber, G. F. The metastasis gene osteopontin: a candidate target for cancer therapy. *Biochim. Biophys. Acta* 1552: 61–85.
39. Senger, D. R., B. B. Asch, B. D. Smith, C. A. Perruzzi, and H. F. Dvorak. 1983. A secreted phosphoprotein marker for neoplastic transformation of both epithelial and fibroblastic cells. *Nature* 302: 714–715.
40. Senger, D. R., C. A. Perruzzi, C. F. Gracey, A. Papadopoulos, and D. G. Tenen. 1988. Secreted phosphoproteins associated with neoplastic transformation: close homology with plasma proteins cleaved during blood coagulation. *Cancer Res.* 48: 5770–5774.
41. Bautista, D. S., J. W. Xuan, C. Hota, A. F. Chambers, and J. F. Harris. 1994. Inhibition of Arg-Gly-Asp (RGD)-mediated cell adhesion to osteopontin by a monoclonal antibody against osteopontin. *J. Biol. Chem.* 269: 23280–23285.
42. Hijiya, N., M. Setoguchi, K. Matsuura, Y. Higuchi, S. Akizuki, and S. Yamamoto. 1994. Cloning and characterization of the human osteopontin gene and its promoter. *Biochem. J.* 303: 255–262.